Study of Static Recrystallization Behaviors of GCr15 Steel Under Two-Pass Hot Compression Deformation

Huajie Mao, Rui Zhang, Lin Hua, and Fei Yin

In order to study the static recrystallization behavior of GCr15 steel during hot deformation process, two-pass hot compression experiments were conducted on Gleeble-3500 thermo-simulation system at the test temperatures from 850 to 1150 °C strain rate from 0.01 to 1 s^{-1}, strain from 0.05 to 0.15 and inter-stage delay time from 1 to 100 s, respectively. The effects of temperature, strain rate and strain on static recrystallization of GCr15 steel were discussed in details. And the kinetic equations, in which the tension-time index n was 0.35 and the activation energy Q was 225.86 kJ/mol, were proposed. The comparison between the experimental results and predicted results was performed and the research results indicated that the effects of deformation parameters on the static recrystallization in multi-stage hot deformation are significant. The predicted results are in good agreement with the experimental ones, which indicates that the proposed kinetic equations can give an accurate estimate of the static recrystallization behaviors and microstructural evolutions for GCr15 steel.

1. Introduction

With the development of simulation and analysis, finite element method (FEM) has been widely and successfully used to analyze and optimize the materials forming processes. And the accuracy of the simulated results greatly depends on the accuracy of the mathematical models, thus setting up accurate constitutive models for processing materials is the key to the success of simulation and analysis.

Lin et al. carried out the basic research on low alloy steel static recrystallization, summarized the relationship between deformation conditions and static recrystallization percentage and established the static recrystallization kinetics equation (Ref 1). Yue et al. developed a mathematical model to predict the austenite grain size of GCr15 during thermal process (Ref 2). Yin et al. developed the constitutive model for flow behavior of GCr15 steel (Ref 3) and they formulated the constitutive equations for flow stress, austenite grain growth and dynamic recrystallization of GCr15 steel by linear regression method and genetic algorithm based on the results of

stress-strain curves and metallographic analysis (Ref 4). Wang et al. studied the work hardening and dynamic soften behavior of 20MnNiMo steel, then set up the constitutive equations of the flow stress of the steel, defined the critical condition of the steel dynamic recrystallization, and made qualitative description of the relationship between dynamic recrystallization activation energy, Z values and the strain, at last pointed out that the coarse grains is the main reason for increased activation energy in the high strain and low Z value (Ref 5). Cheng et al. obtained the recrystallization activation energy and the relationship between dynamic recrystallization critical strain and peak strain, which based on the studies of different stress-strain curves of high-niobium alloy steel deformation processes (Ref 6). Castan et al. pointed out that two types of dynamic recrystallization may operate during hot deformation in Fe-8% Al alloy: the alloy undergoes discontinuous dynamic recrystallization at high temperature and high strain rate, whereas continuous dynamic recrystallization occurs at lower temperature and strain rate through the application of backscattered electron spectra study (Ref 7). Chen et al. developed the dynamic recrystallization kinetics equation of 42CrMo (Ref 8). Masoud Mirzaee et al. made the study of chemical precipitation and dynamic recrystallization of 26NiCrMoV steel, obtained the recrystallization activation energy 437 kJ/mol and explained the reason the abnormal curve of flow stress below 1000 °C (Ref 9). Mateo et al. studied the effect of vanadium on micro-alloyed steel static recrystallization (Ref 10). Lin et al. studied the hot deformation process of 42CrMo steel and summed up the corresponding model forecast for the change of the flow stress under the conditions of high temperature and high strain, and on this basis for 42CrMo steel under different deformation temperature stress the inequality of the distribution of the strain were described in detail, they also finished the establishment of a computer simulation model of stress and strain in the hot forging process and microstructure evolution of 42CrMo steel (Ref 11-15). Yue et al. made a preliminary study on the GCr15 dynamic recrystallization (Ref 16).

Huajie Mao, School of Materials Science and Engineering, Wuhan University of Technology, Wuhan 430070, China and Hubei Key Laboratory of Advanced Technology for Automotive Components, Wuhan, 430070, China; **Rui Zhang**, School of Materials Science and Engineering, Wuhan University of Technology, Wuhan 430070, China; and **Lin Hua** and **Fei Yin**, School of Automotive Engineering, Wuhan University of Technology, Wuhan 430070, China and Hubei Key Laboratory of Advanced Technology for Automotive Components, Wuhan 430070, China. Contact e-mail: huajiem@outlook.com.

The metal theory shows that the mechanical properties of metal depends on the microstructure of materials, static recrystallization behavior has a significant impact on the microstructure. Accurate description of the recrystallization behavior can predict the microstructure of products under specific process. Now many scholars use these recrystallization models to simulate the microstructure evolution behavior in the deformation. GCr15 steel is one of the most commonly used bearing steels. There are some researches about its austenite grain growth and dynamic recrystallization behaviors, but also few about its static recrystallization behavior. Therefore, we choose GCr15 steel as research object to study its static recrystallization behavior, which will provide the basic static recrystallization parameters for microstructure evolution simulation of GCr15 steel during hot deformation process.

In this paper, the static recrystallization behavior of GCr15 steel and the material constants of static recrystallization kinetic equation that is connected with deformation temperature, strain rate, strain and initial grain size were studied experimentally. Gleeble-3500 thermo-simulation system was used to study the static recrystallization behavior of GCr15 steel. The true stress-strain curves for GCr15 steel under different deformation temperatures from 850 to 1150 °C strain rates from 0.01 to 1 s^{-1} and strain from 0.05 to 0.15 were recorded, respectively. According to the curves, 'offset method', linear fitting and regression analysis were used to determine the softening fraction and solve the static recrystallization kinetic equations.

2. Materials and Experimental Procedure

The chemical composition of the continuous casting slab GCr15 steel used in this study is shown in Table 1, by lathing, wire-electrode cutting and grinding, specimens with the diameter of 8 mm and height of 12 mm were used according to the experimental requirements of the Gleeble-3500 thermo-simulation analysis system.

To clarify the effect of different factors on the static recrystallization, four groups of experiments were carried out as shown below.

The graphite sheet was affixed at both ends of the specimen to prevent the adhesions between the surface of the specimen and the surface of the die at high temperature.

Group A: In order to investigate the effect of deformation temperature on static recrystallization, during the tow-pass hot compression test, different test temperatures T (850, 950, 1000, 150 °C with specific strain rate and $\dot{\varepsilon}$ 0.1 s^{-1}

Table 1 Chemical composition of the GCr15 steel used in this study (wt.%)

C	0.96
S	0.006
P	0.013
Mn	0.36
Si	0.19
Cr	1.46
Mo	0.02
Cu	0.06
Ni	0.08
Fe	Balance

and strain ε 0.1 were performed. And the inter-stage delay time t was set as 1, 5, 10, 30, 100 s.

Group B: In order to investigate the effect of strain rate on static recrystallization, hot compression tests with different strain rate $\dot{\varepsilon}$ (0.01, 0.1, 0.5, 1 s^{-1}) and specific temperature T 1000 °C and strain ε 0.1 were performed. And the inter-stage delay time t was set as 1, 5, 10, 30, 100 s.

Group C: In order to investigate the effect of strain on static recrystallization, hot compression tests with different strains ε under strain rate $\dot{\varepsilon}$ 0.1 s^{-1} and temperature T 1000 °C In hot deformation, dynamic recrystallization cannot be activated until the energy accumulation reaching a threshold value which is called critical strain. The method to determine the critical strain of GCr15 steel was described in Ref 4. When strain rate $\dot{\varepsilon}$ 0.1 s^{-1} and temperature T 1000 °C the critical strain is 0.167. So we choose a reduction of 0.05, 0.1, and 0.15 in specimen height, the strain for each deformation was kept below the critical strain. And the inter-stage delay time t was set as 1, 5, 10, 30, 100 s.

Group D: In order to investigate the effect of initial grain size on static recrystallization, before deformation, specimens were heated to 950, 1000, 150 °C, respectively, and keep for 300 s to get different initial grain size. Test temperature T 1000 °C $\dot{\varepsilon}$ 0.1 s^{-1} and strain ε 0.1 were used in two-pass hot compression tests. And the inter-stage delay time t was set as 1, 5, 10, 30, 100 s.

For Group A, B, and C, the specimen were heated to 1200 °C at the heating rate of 5 °C/s and held for 400 s. Then, the specimens were cooled to the specified temperature at 5 °C/s and held for 60 s to eliminate thermal gradients before the first deformation, the specimens were held at the deformation temperature for the inter-stage delay time of 1-100 s according to the experimental design to enable static recrystallization to progress, a second deformation was then applied to measure the amount of softening, the deformation temperatures, strain rates and the strains were same to the first and second deformations, and then the specimens were rapidly quenched in water and the experimental routine can be seen in as shown in Fig. 1(a). For Group D, the specimens were heated to 950, 1000, 1150 °C at the heating rate of 5 °C/s and held for 300 s. Then, the specimens were cooled to the specified temperature at 5 °C/s and held for 60 s to eliminate thermal gradients. Then two-pass compression conducted at $T = 950$ °C $\dot{\varepsilon} = 0.1$ s^{-1} $\varepsilon = 0.1$, $t = 1, 5, 10, 30, 100$ s, and then the specimens were rapidly quenched in water and the experimental routine can be seen as shown in Fig. 1(b).

3. Results and Discussion

### 3.1 Stress-Strain Curves in Inter-Stage Hot Compression

Typical true stress-strain curves obtained from the two-pass hot compression test of GCr15 steel are depicted in Fig. 2. It is obvious that the extent of static softening increased and the yield stress of the second compression decreases when the inter-stage delay time is increased, which shows the softening because of static recovery and recrystallization of materials. Similar results were obtained under other test conditions. Besides, the curve with the inter-stage delay time of 30 s overlaps that with the inter-stage delay time of 100 s, which
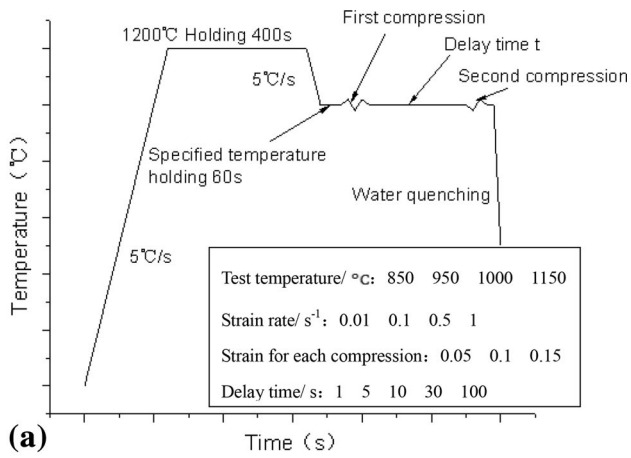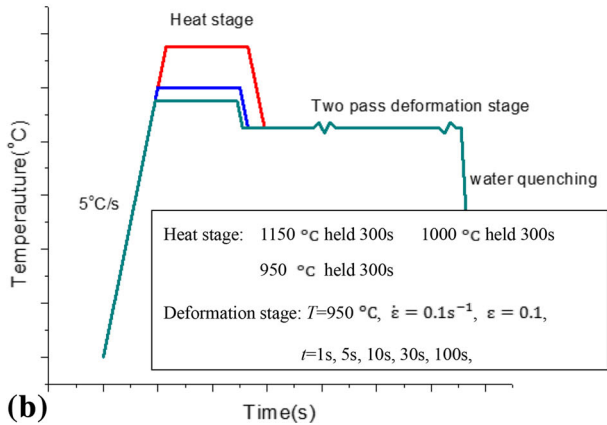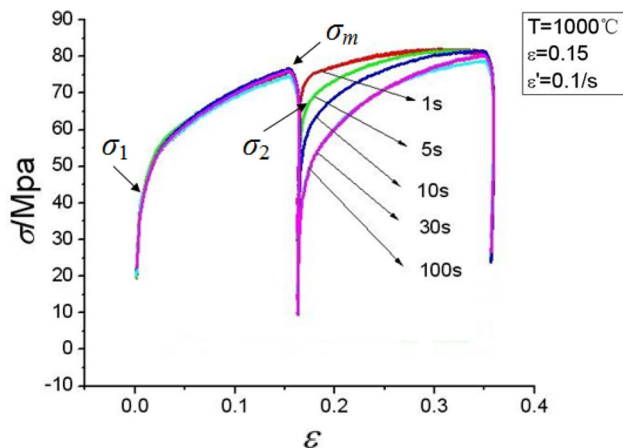
Fig. 1 Schematic diagram of experimental procedure (a) for Group A, B, C (b) for Group D

Fig. 2 Typical true stress-strain curve

indicates the complete static recrystallization happened under the experimental conditions when the inter-stage delay time is 30 s.

3.2 Determination of the Softening Fraction and Static Recrystallization Fraction

The interrupted hot compression tests are based on the principle that the yield stress at high temperatures is sensitive of the structural changes. In this study, the 0.2% offset yield strength was used to determine the softening due to static recrystallization and recovery. So the 'offset method' was used to determine the softening fraction, as the formula below:

$$F_s = (\sigma_m - \sigma_2)/(\sigma_m - \sigma_1), \qquad (\text{Eq 1})$$

where σ_m is the flow stress at the interruption, σ_1 and σ_2 are the offset stresses at the first compression and the second compression, respectively.

Assuming that the recrystallization starts at some critical softening fraction value, which is 0.2, the static recrystallization fraction, φ_s can be determined from the softening data using the following formula:

$$\varphi_s = \frac{(F_S - 0.2)}{1 - 0.2} = (F_S - 0.2)/0.8. \qquad (\text{Eq 2})$$

3.3 Effects of Deformation Parameters on Static Recrystallization Fraction

To illustrate the effects of the process parameters on the static recrystallization of GCr15 steel, the stress-strain curves at different deformation temperatures, strain rates and strains were recorded, respectively. Then data have been chosen to calculate to make $\varphi_s - \ln(t)$ images as shown in Fig. 3 by the offset method described above.

3.3.1 Effects of Deformation Temperature. Figure 3(a) shows the relationship between the static recrystallization fraction and the inter-stage delay time under different deformation temperatures at the strain rate of 0.1 s^{-1} and strain of 0.1. It can be seen from Fig. 3(a) that the effects of deformation temperature on static recrystallization are significant. The static recrystallization fraction increases with the increase of the deformation temperature. At the beginning, the value of static recrystallization fraction under the deformation temperature of 1150 °C is already over 60% while the value of static recrystallization fraction under the deformation temperature of 850 °C is just reach 60% at the delay time of 100 s. This result indicates that the static recrystallization cannot completely occur under low temperature while can conduct much faster under high temperature. As the static recrystallization is thermally activated, the fraction increases with the increase of the deformation temperature.

3.3.2 Effects of Strain Rate. The effects of strain rate on static recrystallization were studied in this section. Figure 3(b) shows the variation of static recrystallization fraction with inter-stage delay time and different strain rates at the deformation temperature of 1000 °C and strain of 0.1. The static recrystallization curves indicate that the effect of strain rate on the fraction of static recrystallization is less than that of the temperature. With the delay time of 100 s during experiment, the value of static recrystallization fraction under the strain rate of 0.5 s^{-1} is as much as that under the strain rate of 1 s^{-1}. It is evident that the recrystallization is accelerated significantly when the strain rate is increased: the static recrystallization fractions with the strain rate of 1 s^{-1} are larger than those with lower strain rates of 0.01 s^{-1}. This is due to the higher strain energy stored in the deformation block under high strain rate conditions. Then, the reduced extent of dynamic recovery occurring at higher strain rates in turn produces a higher dislocation density and increases the driving force for recrystallization.

3.3.3 Effects of Strain. The relationship between the static recrystallization fraction and inter-stage delay time under different pre-strain conditions (a reduction of 0.05, 0.1, and 0.15 of specimen height in the first deformation) is shown in Fig. 3(c).
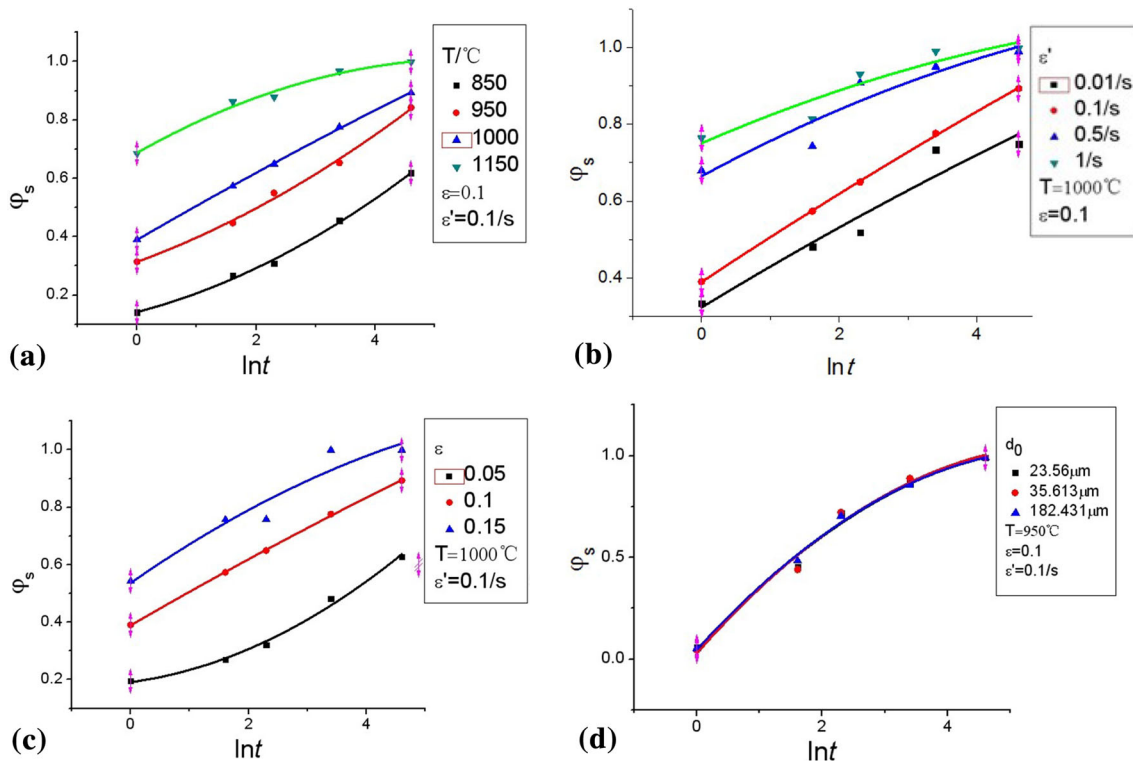
Fig. 3 Dependence of static recrystallization fraction on (a) deformation temperature (b) strain rate (c) deformation degree (d) initial grain size

It can be found that the static recrystallization fraction and the rate of static recrystallization increase with the increase of strain in the first stage. For the relatively low pre-strain conditions such as 0.05, the rate of static recrystallization is small, which indicates that the static recrystallization under the relatively low pre-strain conditions mainly results from the recovery. However, for the relatively high pre-strain conditions such as 0.1 and 0.15, the rate of softening is larger, because the static recrystallization takes over recovery and proceeds more rapidly, and movement of new grain boundaries is a more rapid way to remove dislocations than dislocation interaction.

3.3.4 Effects of Initial Grain Size. The effects of initial on static recrystallization were studied in this section. Figure 3(d) shows the variation of static recrystallization fractions with inter-stage delay time and different initial grain size at the deformation temperature of 950 °C strain rate of 0.1 s^{-1} and strain of 0.1. The curves are almost overlap, which indicates that the initial grain size has little effect on static recrystallization of GCr15 steel.

3.4 Modeling the Kinetics of Static Recrystallization

The kinetics of static recrystallization is usually defined by an Avrami equation:

$$\varphi_s = 1 - \exp\left[-0.693\left(\frac{t}{t_{0.5}}\right)^n\right], \tag{Eq 3}$$

where n is material dependent constant, $t_{0.5}$ is the time for the recrystallizing volumetric fraction of 50%. The expression most widely used for this parameter is

$$t_{0.5} = Ad_0^h \varepsilon^p \dot{\varepsilon} \exp\left[Q/(RT)\right], \tag{Eq 4}$$

where A, p, q and h are material dependent constants, ε is the true strain, $\dot{\varepsilon}$ is the strain rate, R is the gas constant (J/mol K)

and the value of R is 8.314 in this study, T is the absolute temperature (K), Q is the apparent activation energy of recrystallization (kJ/mol) and d_0 is the initial austenite grain size (µm)

3.4.1 Determination of n. Take the logarithm of both sides of Eq 3 twice:

$$\ln\left(\ln\left(\frac{1}{1 - \varphi_s}\right)\right) = \ln 0.693 + n\ln t - n\ln t_{0.5}. \tag{Eq 5}$$

By substituting the values of calculated from Eq 2 and corresponding inter-stage delay time under different test conditions into Eq 5, the relationships between the static recrystallization fraction and inter-stage delay time: $\ln(\ln(\frac{1}{1-\varphi_s})) - \ln(t)$ can be obtained as shown in Fig. 4 by linear fitting and regression analysis, from which, it is easy to evaluate the average value of n as 0.35.

3.4.2 Determination of the Dependence of $t_{0.5}$ on the Deformation Parameters. Take the logarithm of both sides of Eq 4:

$$\ln t_{0.5} = \ln A + h\ln d_0 + p\ln \varepsilon + q\ln \dot{\varepsilon} + Q/(RT). \tag{Eq 6}$$

From the relationships between φ_s and corresponding inter-stage delay time, the values of $t_{0.5}$ under different test conditions can be derived.

Then, by substituting the values of $t_{0.5}$ and deformation temperatures into Eq 6, the relationship between $\ln t_{0.5}$ and $[(1/T)*1000]$ can be obtained as shown in Fig. 5 by linear fitting and regression analysis. The mean value of the slope for the group of the straight lines is Q/R and $R = 8.314$ given, so the Q can be calculated as 225.86 kJ/mol.
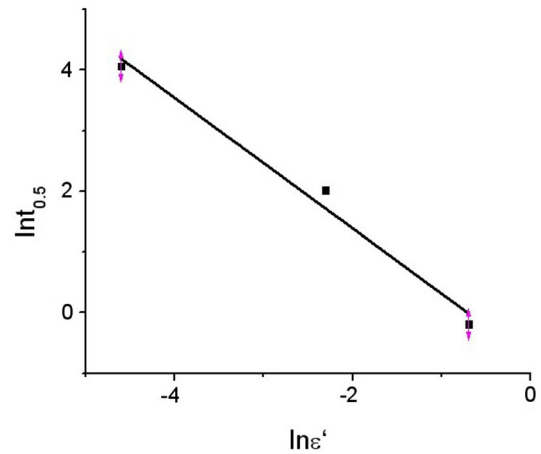
By substituting the values of $t_{0.5}$ and different pre-strain into Eq 6, the relationship between $\ln t_{0.5}$ and $\ln \varepsilon$ can be obtained as shown in Fig. 6 by linear fitting and regression analysis. The
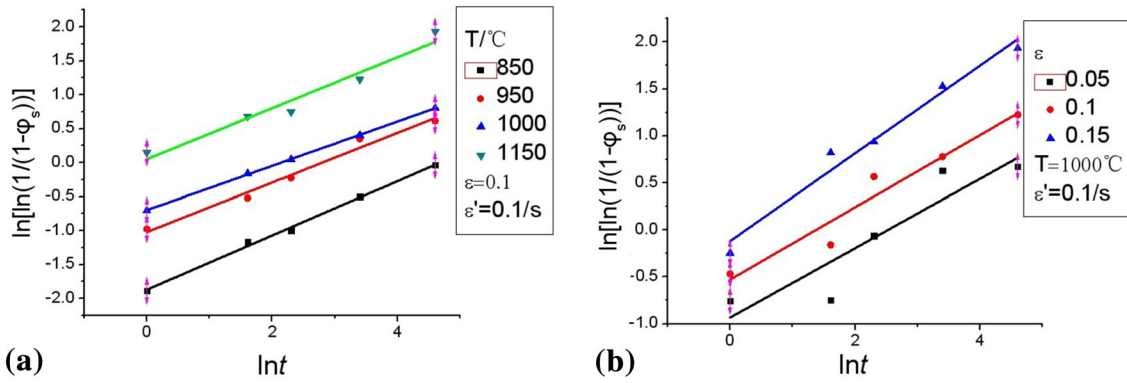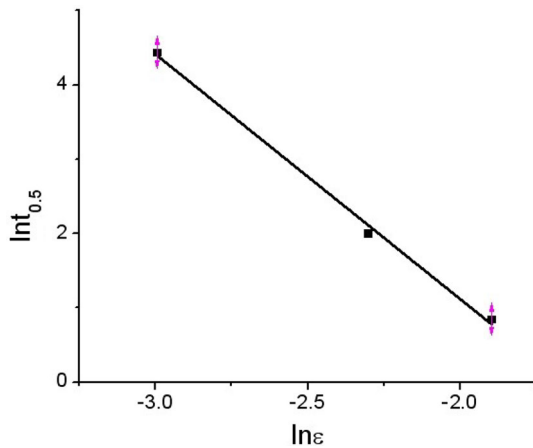
Fig. 4 Relationships between $\ln\left(\ln\left(\frac{1}{1-\varphi_s}\right)\right)$ and $\ln t$ under (a) different deformation temperature (b) different deformation degree
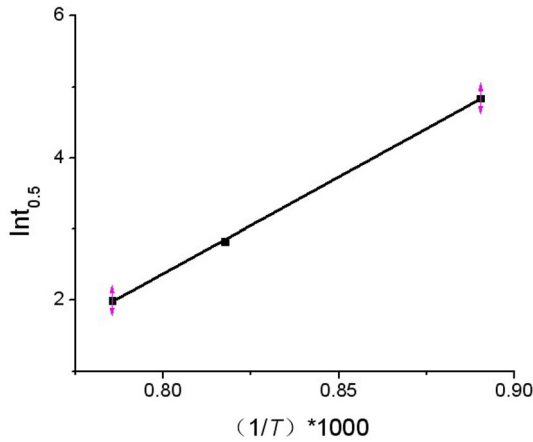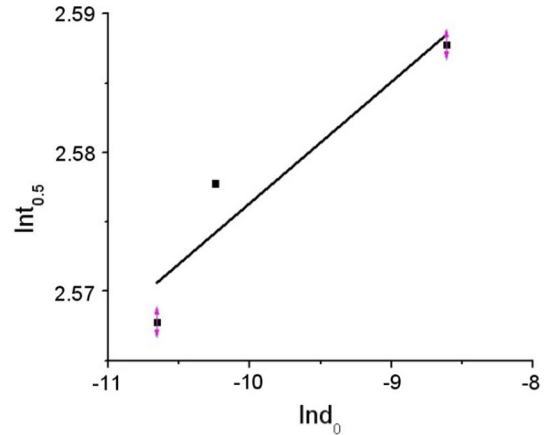

Fig. 5 Relationships between $\ln t_{0.5}$ and $[(1/T)*1000]$

Fig. 7 Relationships between $\ln t_{0.5}$ and $\ln\dot{\varepsilon}$

Fig. 6 Relationships between $\ln t_{0.5}$ and $\ln\varepsilon$

**Fig. 8** Relationships between $\ln t_{0.5}$ and $\ln d_0$

mean value of the slope for the group of the straight lines is p and it is easy to evaluate $p = -3.29$.

Similarly, shown in Fig. 7 and 8, the values of material dependent constant $q = -1.07$ and $h = 0.01$. Additionally, the constant A can be easily derived as 2.04×10^{-13} based on the obtained material dependent constants above.

Then, the kinetics of static recrystallization for GCr15 steel can be represented as the following equations:

$$\varphi_s = 1 - \exp\left[-0.693\left(\frac{t}{t_{0.5}}\right)^{0.35}\right], \tag{Eq 7}$$

$$t_{0.5} = 2.04 \times 10^{-13} d_0^{0.01} \varepsilon^{-3.29} \dot{\varepsilon}^{-1.07} \exp[225860/(RT)]. \tag{Eq 8}$$
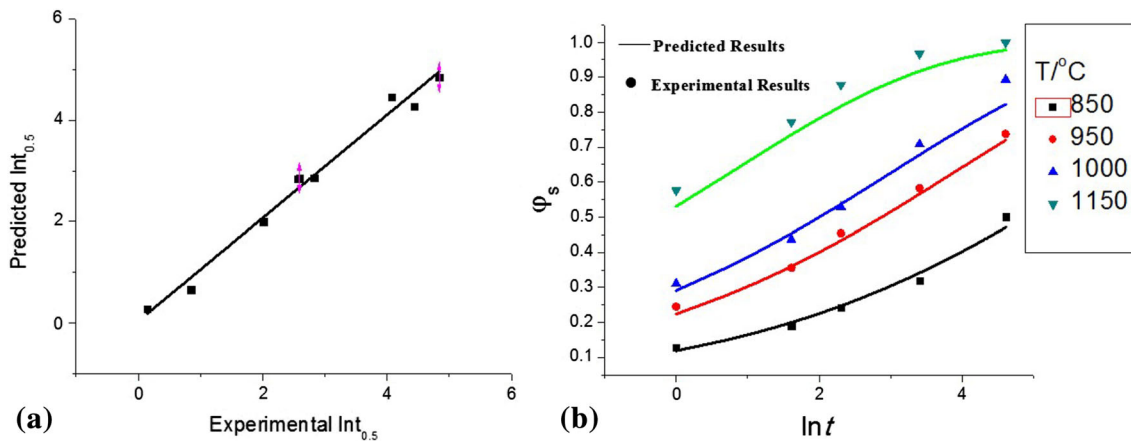
Fig. 9 Comparison between the experimental and predicted results (a) for the time for the recrystallizing volumetric fraction of 50% (b) for values of static recrystallization fraction

3.5 Comparison Between the Experimental and Predicted Results

In order to verify the developed kinetic equations, for the static recrystallization of GCr15 steel, comparisons between the experimental and predicted results were carried out. Figure 9 shows the comparisons between the experimental and predicted values of $t_{0.5}$ and static recrystallization fraction. It can be found that all the predicted results are in good agreement with the experimental ones, indicating that the proposed kinetic equations can give an accurate and precise estimate of the softening behaviors and microstructural evolutions for GCr15 steel, during metal forming process.

4. Conclusions

In this study, the effects of deformation parameters on the softening in two-pass hot deformation of GCr15 steel were studied. And the fundamental understanding of the static softening behaviors during multi-stage hot deformation of GCr15 steel was obtained. Research results indicate that the softening fractions rapidly increase with the increase of the deformation temperature, strain rate and strain. And the effect of the temperature on fraction of static recrystallization is greater than that of other process parameters.

In addition, the kinetic equations of the static recrystallization behaviors for the two-pass hot deformed GCr15 steel were developed. Good agreement between the experimental and predicted results indicates that the proposed kinetic equations can give an accurate and precise estimate of the softening behaviors and microstructural evolutions for GCr15 steel during metal forming process.

Acknowledgments

References

1. Y.C. Lin, M.S. Chen, and J. Zhong, Study of Static Recrystallization Kinetics in a Low Alloy Steel, *Comput. Mater. Sci.*, 2008, **44**, p 316–321
2. C.X. Yue, L.W. Zhang, and S.L. Liao, Mathematical Models for Predicting the Austenite Grain Size in Hot Working of GCr15 Steel, *Comput. Mater. Sci.*, 2009, **45**, p 462–466
3. F. Yin, L. Hua, H.J. Mao et al., Constitutive Modeling for Flow Behavior of GCr15 Steel Under Hot Compression Experiments, *Mater. Des.*, 2013, **43**, p 393–401
4. F. Yin, L. Hua, H. Mao, X. Han, D. Qian, and R. Zhang, Microstructural Modeling and Simulation for GCr15 Steel During Elevated Temperature Deformation, *Mater. Des.*, 2014, **55**, p 560–573
5. M.H. Wang, Y.F. Li, W.H. Wang et al., Quantitative Analysis of Work Hardening and Dynamic Softening Behavior of Low Carbon Alloy Steel Based on the Flow Stress, *Mater. Des.*, 2013, **45**, p 384–392
6. L. Cheng, H. Chang, B. Tang et al., Deformation and Dynamic Recrystallization Behavior of a High Nb Containing TiAl Alloy, *J. Alloy. Compd.*, 2013, **552**, p 363–369
7. C. Castana, F. Montheillet, and A. Perlade, Dynamic Recrystallization Mechanisms of an Fe-8% Al Low Density Steel Under Hot Rolling Conditions, *Scripta Mater.*, 2013, **68**, p 360–364
8. M.S. Chen, Y.C. Lin, and X.S. Ma, The Kinetics of Dynamic Recrystallization of 42CrMo Steel, *Mater. Sci. Eng. A*, 2012, **556**, p 260–266
9. M. Mirzaee, H. Keshmiri, G.R. Ebrahimi et al., Dynamic Recrystallization and Precipitation in Low Carbon Low Alloy Steel 26NiCrMoV14-5, *Mater. Sci. Eng. A*, 2012, **551**, p 25–31
10. C.G. Mateo, B. López, and J.M. Rodriguez-Ibabe, Static Recrystallization Kinetics in Warm Worked Vanadium Microalloyed Steels, *Mater. Sci. Eng. A*, 2001, **303**, p 216–225
11. Y.C. Lin, M.S. Chen, and J. Zhong, Prediction of 42CrMo Steel Flow Stress at High Temperature and Strain Rate, *Mech. Res. Commun.*, 2008, **35**, p 142–150
12. Y.C. Lin, M.S. Chen, and J. Zhang, Modeling of Flow Stress of 42CrMo Steel Under Hot Compression, *Mater. Sci. Eng. A*, 2009, **499**, p 88–92
13. Y.C. Lin, M.S. Chen, and J. Zhong, Effects of Deformation Temperatures on Stress/Strain Distribution and Microstructural Evolution of Deformed 42CrMo Steel, *Mater. Des.*, 2009, **30**, p 908–913
14. Y.C. Lin, M.S. Chen, and J. Zhong, Numerical Simulation for Stress/Strain Distribution and Microstructural Evolution in 42CrMo Steel During Hot Upsetting Process, *Comput. Mater. Sci.*, 2008, **43**, p 1117–1122
15. Y.C. Lin, M.S. Chen, and J. Zhong, Constitutive Modeling for Elevated Temperature Flow Behavior of 42CrMo Steel, *Comput. Mater. Sci.*, 2008, **42**, p 470–477
16. C.X. Yue, L.W. Zhang, S.L. Liao et al., Research on the Dynamic Recrystallization Behavior of GCr15 Steel, *Mater. Sci. Eng. A*, 2009, **499**, p 177–181